2024 IEEE/RSJ International Conference on Intelligent Robots and Systems (IROS)
October 14-18, 2024. Abu Dhabi, UAE

Optimal Sensing in Soft Pneumatic Actuators via Stretchable Optical Waveguides

Faisal Aljaber[1], Ahmed Hassan[2], Ivan Vitanov and Noora Almeadadi[1], Hind AlHajri[1], Sara AlEnazi[1], Rashid Al-marri[1], Kaspar Althoefer[3] and Pilsung Choe

***Abstract*— Stretchable optical waveguides have been explored as a route to enhancing the sensing capabilities of soft actuators. Certain properties and qualities they possess recommend them for this task – their biological plausibility, compliance, low power consumption, and heightened responsiveness to external stimuli. Though well regarded for their efficiency, their practical application warrants a more detailed examination as regards their sensitivity, robustness, and resilience when integrated with various manipulators. There is a dearth of comprehensive, wide-ranging studies that investigate the relationship between soft sensors and actuators, both in terms of integration and sensor performance – the present study endeavours to fill this void. Here we present a series of findings as to the interdependent relationship at the nexus of soft actuator sensorisation, sensitivity and responsiveness. Building on our previous work and prior waveguide designs, we examine the influence of sensor location and placement along the deformation axis on responsiveness, repeatability, and longevity. Location is key as, during bending, one side experiences tension, while the other compression. Placement is identified as 'straight' or 'loose'. Three PneuNet-based actuators were used in three design configurations: one without any additional modifications, one with a few rigid exoskeleton reinforcements, and one covered fully with rigid exoskeleton reinforcements. The purpose of applying the exoskeletons is to hold the waveguide-based sensors and to suppress any bubble formation. Each design enables the straightforward integration of sensors, so that the relationship between soft actuator design and sensor performance is easy to assess when applying various pressure intakes (from 0 to 7.1 psi) to actuate the bending motion.**

I. INTRODUCTION

Soft robots are increasingly coming to the forefront as a consequence of their bio-realism, compatibility, compliance, and low cost, in addition to the fact that they are inherently safe and simple to control[1], [2], [3], [4], [5]. They possess intrinsic flexibility and adaptability as opposed to their fully rigid-bodied counterparts and can morph into different shapes as well as mimic an array of motions characteristic of aquatic and reptilian organisms[1], [2], [3], [4], [5]. Equipping them with enhanced sensing is vital for all manner of applications across a range of industries.

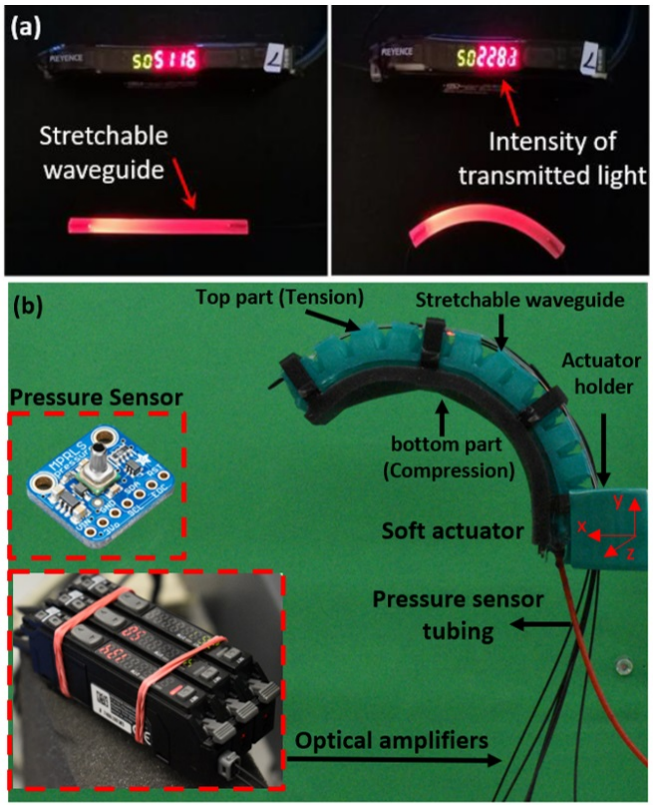

Fig. 1. a) The waveguides (sensing elements) responsiveness is being tested by using the optical amplifiers. b) The experimental setup that involves optical amplifiers, pressure sensor, and the soft actuator with the compression and the tension sides pointed out.

However, integrating sensors into soft actuators is not randomly done has, until now, been largely dictated by design constraints or convenience, without much consideration given to easy detachment, in the case of sensor malfunction, or the need for urgent replacement. Actuator sensorisation and the sensor location within the actuator contribute directly to the longevity and the accuracy of the sensor in the long run.

There have been a lot of studies and examples where sensors were placed in a certain way to serve a specific intended application or because the actuator design restricted the options in which the integration could happen. Zhao et al. have introduced two sensorised soft actuators using optical sensing in [6] and [7]. One of the soft actuators is an

This work was supported by KINDI Centre for Computing, Robotics Lab, Department of Mechanical and Indstrial Engineering, Qatar University.

[1]Authors are with College of Engineering, Mechanical and Industrial Engineering, Qatar University, Qatar.

[2]Author is with College of Engineering, Design and Physical Sciences, Brunel University, London, United Kingdom.

[3]Author is with Queen Mary University of London, London, United Kingdom. f.aljaber@qu.edu.qa, ahmed.hassan@brunel.ac.uk, ivvitanov@yahoo.co.uk, k.Althoefer@qmul.ac.uk

orthotic glove embedded with abraded optical fibres to which laser abrasion is administered at seven pairs of approximately equidistant points along both sides of a naked U-shape [6]. The abrasion is administered along the compression side to simulate the increase in light intensity while bending the fingers[6]. The second design (named optoelectronically innervated soft prosthetic hand) detailed in [7] utilised larger waveguides than the first, making it overall design which makes the whole design relatively larger than the design presented in [6].

Meerbeek et al. introduced a soft optoelectronic sensory foam with proprioception, utilising an array of 30 embedded inside a soft structure to sense bending and twisting [8]. Jamil et al. introduced a sensorised PneuNet-based soft actuator with rigid reinforcement that encapsulates a rigid optical fibre to sense bending, and soft optical sensors to sense forces when the actuator comes in contact with different objects [9]. Godaba et al. presented a comparison between two different types of sensors – pressure-insensitive abraded optical fibres and pressure-sensitive waveguides – to sense bending in PneuNet soft actuators [10], [11], [12].

Shi et al. presented an extensive review of soft optical-based sensors in their analysis of shape sensing techniques [13], in which they examine the implementation of different sensing modalities and their integration with continuum robots. The use of optical-based sensors utilising fibre Bragg gratings (FBGs) in medical robotics is discussed in detail, with a focus on the challenges as we move from stiff needle shapes to highly flexible actuators [13]. This work, however, fails to consider the effect of hyper-redundant robot deformation on waveguide sensors [13]. Both Shi et al. and Henken et al. have reported an error analysis concerning data acquisition, signal, and shape and curvature estimation. This leads to improving the placement of each sensor and increasing the number of placed sensors along the length of the continuum robot [13], [14].

The studies mentioned above are considered to be essential in their field of contribution, however, these studies do not mention or touch on the process of explaining the design considerations that predicate sensor location choice or predetermine the number of sensors necessary. Zhao et al.'s soft sensors are mostly embedded within the soft actuated fingers, making it hard to replace or repair damaged sensors [6], [7]. Godaba et al. only applied bending to a small section of their soft actuator, and the bending was not tested on a stretchable waveguide by way of comparison with the abraded optical fibre [10]. Jamil et al. used a single rigid optical fibre to sense the deformation due to bending in the soft actuator. This is clearly limiting, as a single sensor cannot give a true representation of the bending effect, as different parts of the actuator will experience the bending differently [9].

In this study we try to bridge the gap on stretchable waveguides, in terms of their integration, placement, and localisation within a soft actuator, this paper aims to address this apparent gap in the literature and body of knowledge, and in so doing, make an attempt at improving the performance of these sensors in relation to the above parameters on the basis of empirical findings and methodological rigour. Utilising the novel staggered configuration of our sensor designs already presented in [15], [16], [17], the paper will address the following:

- A practical and easy way to attach and detach soft sensors to soft actuators without wasting materials or having to redesign the actuator.
- The staggered waveguide sensors used in this study are placed and integrated into the soft actuators using two different configurations to widen the sensorisation options (housed sensors and individually placed sensors).
- The location of the sensors with respect to the compression and tension side of the bending soft actuator is investigated and discussed.
- The location of the sensors with respect to the compression and tension side of the bending soft actuator is investigated and discussed.
- Our sensorisation method will demonstrate the advantage of placing multiple sensors along the entire length of the soft actuator.

II. Design Considerations and Fabrication

A. Design Considerations

Before starting the fabrication processes for both the sensors and actuators, several design considerations were identified in order to ensure optimal performance. These design considerations for the sensors are subject to the waveguides' triplet staggered-type configuration, i.e., whether they are housed or individually attached to the soft actuator using an exoskeleton, as Fig. 1 and Fig. 3 show. The waveguides are located either at the top or the bottom of the actuator, depending on the selected sensor configuration to be tested. This is explained in greater detail in section III. All soft actuators' sides are excluded from sensorisation for the following reasons: 1) placing the optical fibres and the waveguides on the side of the actuators might restrict the bending motion and work as an obstacle preventing the actuators from reaching maximal bending; 2) locating the waveguides on the side is redundant, as bending occurs along the z-axis, as Fig 1 shows; 3) the side areas of any actuator only provide enough surface area for a maximum of two waveguides; 4) in any event, only one of the two sides could be sensorised, as optical fibre cables would naturally occupy the reverse side; and 5) the friction caused by optical fibre cables could damage the soft actuators. For the soft silicon pneumatic actuators (SSPAs), the design criteria were as follows: 1) all actuators should be made of the same silicone material mixture to reduce the unknown variables of the experiments and make sure that all actuators hae same mechanical properties such as % elongation and stiffness; 2) the actuators should be relatively lightweight; and 3) the actuator should be able to resist enough pressure to obtain the desired bending.

B. Sensor Fabrication

The fabrication of the waveguide sensors follows the processes presented previously in [10], [15], [17]. To make

the sensing elements, an optical-compatible commercially available clear silicone rubber - Solaris (Smooth-On Inc.) with a refractive index of 1.41 - was used. The Solaris silicone parts A and B were mixed in a 1:1 ratio, and the uncured mixture then injected using a syringe into a clear tube of 1.2 mm diameter with a refractive index ranging between 1.35 and 1.37 that was left for 24 hours at room temperature to cure, as shown in the schematics in Fig 2(a). The waveguides are created by cutting 4.5 cm of the cured Solaris inside the clear tube, a length determined by the fact that approximately three sections make up the the total length of a single bending soft actuator, which is 14.5 cm. The three waveguides are coated with a thin gold layer, in line with the process described in [15]. This is to improve the signal reception and limit the light loss and scattering. A single waveguide is connected to FF-DC-500 optical fibre cable segments by Asahi Kasei, with a core and cladding of 485 µm and 500 µm, respectively, and a total diameter of 1 mm, including the plastic jacket layer.

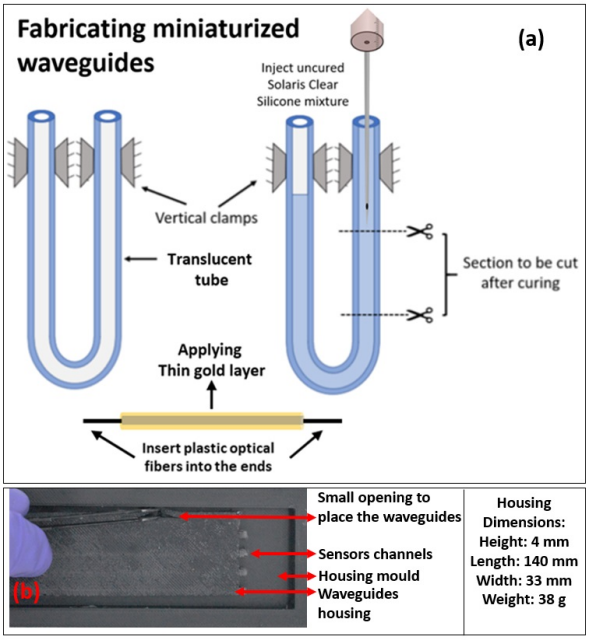

Fig. 2. The fabrication process of making an individual waveguide.

Our novel sensors have waveguides arranged in a staggered fashion, as presented in previous work [15], [17]. These were implemented using two different methods suited for the soft actuators tested in this study. One of the staggered arrangements is a miniaturised version of our sensor presented in [15], [17], which involves the encapsulation of the waveguides (the sensing elements) within soft housing made of a rubber silicone material. The housing is created using equal amounts (60 g) of two distinct rubber silicone materials: Dragon Skin™ 30 and Ecoflex™ 00-50 (Smooth-On Inc.). These are mixed in with a black pigment. The silicone mix is necessary to achieve the desired stiffness without compromising the sensitivity of the sensor, and the black pigment is added to isolate the waveguide from any surrounding interference. The housing mould is 3D-printed using a low-cost plastic filament (PLA) and six equidistant metal rods are placed 5mm apart, to create the channels that encapsulate the waveguides and the optical fibres, as shown in Fig. 2(b). After setting the sensing element in place, extra silicone mixture was poured in to create a total thickness of 4 mm. The housed staggered sensor has a length, width, and height of 140 mm, 33 mm, and 4 mm, respectively, as Fig 2(b) depicts. The second configuration in Fig. 3(a) and 5 depends on the reinforcement of the rigid exoskeleton for soft actuator (SSPAs) sensorisation. A single waveguide is held in place by a number of exoskeleton parts, so the three waveguides will maintain their staggered formation similar to that of the housed waveguides previously introduced in [16]. As shown in Fig. 3(a), each piece of the exoskeleton contains 6 apertures that allow the waveguides to be integrated and held firmly in place. The soft yellow actuator has 12 exoskeletons segments divided into 3, with every 4 exoskeleton segments holding one waveguide; the soft green actuator has 4 exoskeleton segments, where each single waveguide is held by only 2 exoskeleton pieces, as per Fig. 5 shows.

C. PneuNet Soft Actuators

The soft silicon pneumatic actuator (SSPA) is based on a PneuNet actuation technique referred to in previous studies [10], [18], [19] and is a small version of the soft actuator we introduced in [16]. All the soft silicone actuators in this study were made using a mixture of two types of silicone rubber - 70% of Dragon Skin™ 10 FAST and 30% Dragon Skin™ 30. The specific mixture was selected on the basis of the optimal trade-off between higher resistance from the thin air-chambers walls and maximal bending deformation short of causing damage to the actuators. The three actuators used in this study have the same dimensions though a different colour coating to differentiate between them. Two of the actuators have rigid reinforcements applied - the yellow has 12 reinforcement exoskeleton pieces and the green has four (the white has none, as shown in Fig. 5. Both the actuators' inflatable chambers and rigid reinforcement exoskeletons are sealed by a 2 mm layer of silicone material (Dragon Skin™ 10 VERY FAST) for each sealing layer. Figs. 3(a) and 3(b) show the actuators' various integral parts and the dimensions of the soft actuators.

III. Soft Actuator Sensorisation

A. Sensorisation Configurations

Sensorisation configuration refers to the waveguides' triplet arrangement, with and without housing, and their integration into the SSAPs, as in Fig. 3 shows. Sensor placement and location play a major role in the behaviour of the sensor in terms of sensitivity and responsiveness.

B. Sensor placement

Sensor placement here refers to the initial condition under which the three waveguides are integrated into the soft actuators. Fig. 5 shows the different waveguides' placement poses. The green soft actuator in the middle that is partially

reinforced with 4 rigid exoskeletons has the triple staggered waveguide in a loose initial pose. Unlike the green actuator, which has only a few exoskeleton reinforcements, the yellow actuator has all of its air-inflatable chambers reinforced by 12 rigid exoskeleton pices to ensure that the waveguides are placed straight but not stretched, as Fig. **??** shows. The white-coloured actuator is sensorised using the housed sensor configuration, as Fig. 5 shows. The effect of the sensor's placement is explained in full in section V.

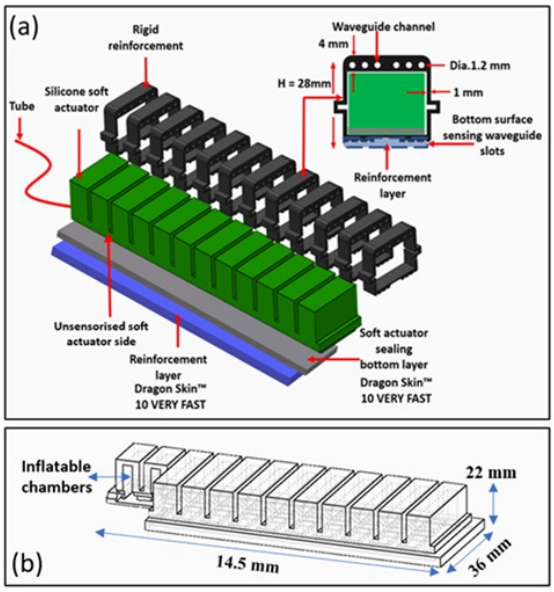

Fig. 3. a) The soft actuator (SSPA) and its various parts with exoskeleton rigid reinforcements. b) The soft actuator dimensions and the air-inflatable chambers.

C. Sensor Location

Sensor location is dependent upon the type of integration it requires, which, in turn, is dependent upon sensor configuration. There are two locations where sensors can be integrated into actuators as Fig 4 shows: 1) the top section of the actuator, which undergoes tension due to the stretching force caused by the pressure, and 2) the bottom section, which is exposed to contraction, since it undergoes compression. The flowcharts in Fig. 4 reference the suitable sensorisation method given the type of sensor integration and location (whether on the tension or compression side). The flowchart in Fig. 4 depicts two paths (A) and (B): for housed waveguide sensorisation and individual waveguides integrated into the soft actuator using exoskeletons, respectively. In path (A) of the flowchart, the staggered housed waveguides cannot be located on the tension side of the actuators because they will restrict and resist the bending motion of the actuator making the compression side the right option. Unlike path (A), in path (B), for the version with exoskeletons, it is impossible to implement the sensor on the compression side because the exoskeleton reinforcement segments will collide, the reinforcement sealing layer placed at the tension side will resist the bending, and the waveguides will bend in an undesired manner, as Fig. 4 shows.

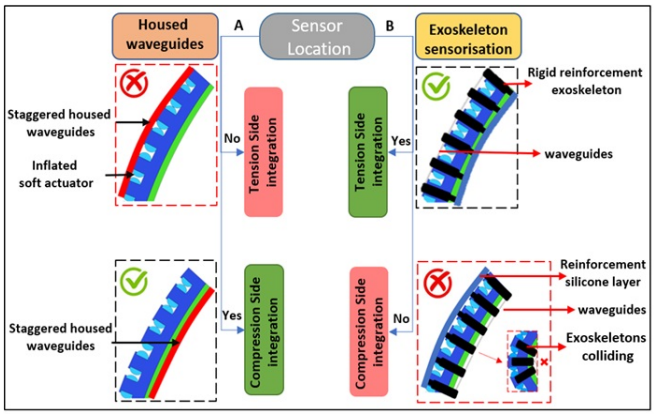

Fig. 4. The flowchart shows the different paths of selecting the proper soft actuator sensorisation in terms of sensor location.

IV. System Setup and Data Acquisition Methodology

The optical fibres connected to both ends of the waveguides (i.e., their sensing elements) are connected to three Keyence FSN11MN optical amplifiers, with in-built light source and photo-detector to acquire voltage signals from the sensors. The optical amplifiers are set at MEGA mode for a standard normal light intensity display that has a response time of 16 ms. The optical amplifiers are used to test individual waveguide responsiveness as shown in Fig. 1(a). It is assumed in this study that the light intensity output is directly proportional to the voltage output signals, and data is acquired through the data recording unit (NI USB DAQ) 6003 provided (DataAcquisition Card, National Instruments) and saved to an Excel sheet. The actuators' gradual bending is controlled using a pressurising system that consists of a pressure sensor, made by Adafruit Industries LLC, that can read absolute pressure from 0 to 25 psi. This is connected to an Arduino microprocessor and pressure regulator to record the pressure data and to ensure consistent gradual pressure increase across all tests. Fig. 1(b) shows the general setup of the experiments with the optical amplifiers and the pressure sensor.

V. Results and Discussion

The recorded signal output of the sensors used to plot the results (i.e., normalised voltage) are the averaged results of three experimental trials. The pressure input for all actuators was kept constant between 0 psi and 7.1 psi, with bending commencing when the pressure exceeded approximately 2 psi. The maximum pressure allowed for all actuators in this study was 7.1 psi, which was sufficient to study the distinct behaviours of each type of sensorisation during the bending experiments. Each SSPA will exhibit different bending angles and curvatures at a certain pressure input due to the type of sensorisation and integration. Fig. 6 shows the results of the white SSPA that has housed waveguides in a staggered configuration sensor located on the compression side of the actuator. The white SSAP seems to bend the least - a consequence of the housing weight resisting the bending. As

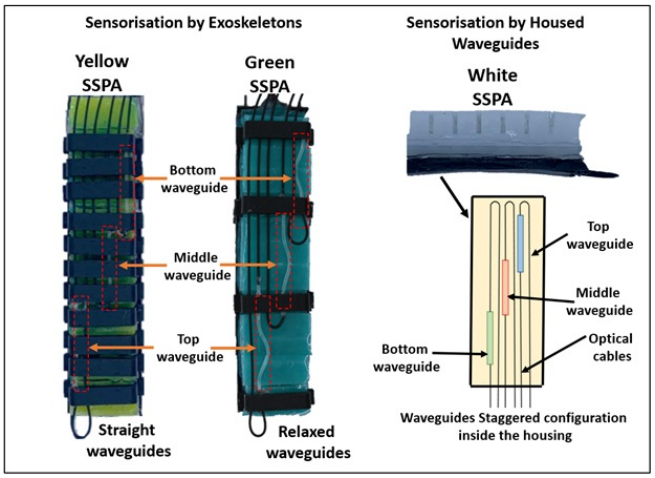

Fig. 5. The types of actuators used in this study: full-exoskeleton integration, limited exoskeleton integration, and no exoskeleton integration.

a result, the maximum bending angle at pressure, as shown at the top section of Fig. 6, is 90° at curvature point 0.15 cm^{-1} and sensor outputs of 0.34 (bottom waveguide), 0.3 (middle waveguide), and 0.45 (top waveguide), with the implication that to achieve a higher bending angle and curvature the pressure has to exceed 7.1 psi. Also, the white SSPA displays uniform behaviour from the first bending initiated by the pressure 2.2 psi denoted by (A) until the maximum bending of 7.1 psi denoted by (G). The sensor output is inversely proportional to the curvature: as the curvature increases, the signals of the sensor (three waveguides) decrease, as shown in the Fig. 6 plot. From pressure input (A) to (B), the white SSPA sensor output signals experience a gradual decrease, and from (B) to (D) the sensor signal outputs exhibit a steep decline and then undergo a gradual decline from (D) to (G). Unlike the white SSAP, the yellow SSAP has a different sensorisation configuration that allows it to behave differently by reducing the weight of the sensors and their location. Fig. 8 shows the plotted results of the sensorised yellow SSPA which is divided into different regions: the grey-shaded region and the white region. In the grey-shaded region that starts from point (A) to point (E) the pressure inputs, the sensor signal outputs, and the curvatures all have a directly proportional relationship: when one increases, the other values increase, too. This behaviour lasts for 5 pressure inputs and then from pressure point (E) to (G): as the pressure and curvature increase, the sensor signal outputs decrease, as Fig. 8 shows. The maximal angle that the yellow SSPA achieves at a maximum pressure of 7.1 psi is approximately 114° at curvature 0.22 cm^{-1} and sensor outputs of 0.33 (bottom waveguide), 0.78 (middle waveguide), and 0.27 (top waveguide). The sensor outputs for both the top and bottom waveguides show great sensitivity compared to the middle waveguide due to the impact of the rigid exoskeletons affecting both waveguides. Like the yellow SSPA, the green SSPA has rigid reinforced exoskeletons; however, there are only 4 compared to the yellow's 12 exoskeleton pieces. Fewer exoskeletons allow the green SSPA to achieve a bending angle of approximately 120° at a maximum pressure of 7.1 psi, a curvature of 0.23 cm^{-1}, and sensor outputs of 0.21 (bottom waveguide), 0.21 (middle waveguide), and 0.21 (top waveguide), as Fig. 7 shows. Compared to the yellow SSPA, the green SSPA has a smaller grey-shaded region as both sensor signal outputs increase proportionally with the bending curvature and the pressure from point (A) to point (C), thereafter steeply declining from point (C) to (G), as Fig. 7 shows.

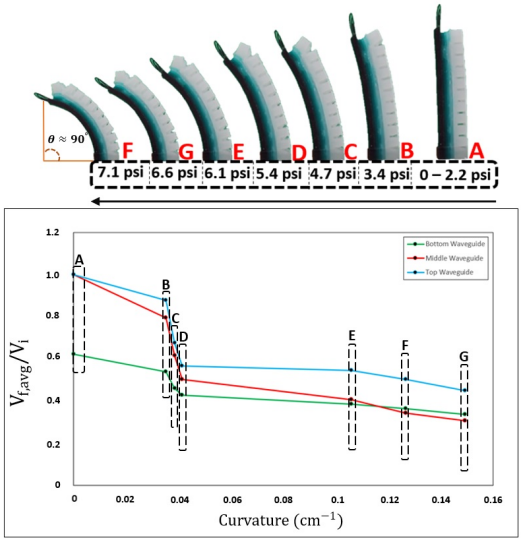

Fig. 6. The bending process of the white SSPA from 0 to 7.1 psi (Top) and the behaviour of the sensor outputs at different pressure points from A to G (Bottom).

The grey-shaded region of the green SSPA is smaller compared to the yellow SSPA due to the direct contact that the waveguides have with air-inflatable chambers that impose extra stress on the sensors, which means making the waveguides decrease in a rapid manner.

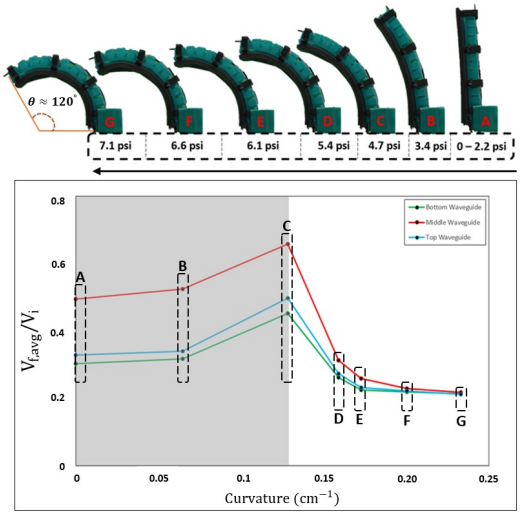

Fig. 7. The bending process of the green SSPA from 0 to 7.1 psi (Top) and the behaviour of the sensor outputs at different pressure points from A to G (Bottom).

It can be noted from the behaviour of the SSPAs that both the green and the yellow SSPAs at the maximal pressure input can bend further in comparison to the white SSPA. Both yellow and green SSPAs being prone to bend more in comparison to the white SSPA due to the sensorisation utilising the rigid exoskeletons technique which does not resist the bending motion like the housed sensors located at the compression side.

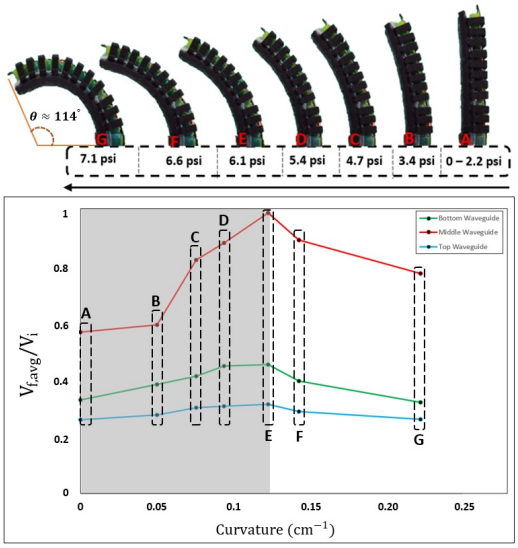

Fig. 8. The bending process of the yellow SSPA from 0 to 7.1 psi (Top) and the behaviour of the sensor outputs at different pressure points from A to G (Bottom).

The white SSPA seems to have more consistent signal outputs over the three waveguides and among the SSPAs, since the waveguides are fully housed and isolated from any external interferences.

VI. Conclusion

We reported on a study of different types of sensorisation using soft stretchable waveguide-based sensors and the effect that location and placement of the sensing elements have on sensing behaviour. Sensorisation located on the tension side or compression side produces two distinct sensor behaviours, each with potential in differing applications. Sensorisation that involves the addition of exoskeletons to hold the waveguides in place can be used to sense different types of motion thanks to the nature of the decoupled behaviour that can be used in expanding and bending soft actuators.

Acknowledgement

The authors would like to thank Mr Mish Toszeghi for proofreading the paper and Qatar University for funding the PhD Research.

References

[1] D. Rus and M. T. Tolley, "Design, fabrication and control of soft robots," *Nature*, vol. 521, no. 7553, pp. 467–475, 2015.

[2] M. Cianchetti, T. Ranzani, G. Gerboni, T. Nanayakkara, K. Althoefer, P. Dasgupta, and A. Menciassi, "Soft robotics technologies to address shortcomings in today's minimally invasive surgery: the stiff-flop approach," *Soft robotics*, vol. 1, no. 2, pp. 122–131, 2014.

[3] S. Kim, C. Laschi, and B. Trimmer, "Soft robotics: a bioinspired evolution in robotics," *Trends in biotechnology*, vol. 31, no. 5, pp. 287–294, 2013.

[4] W. Choi, G. Whitesides, M. Wang, X. Chen, R. Shepherd, A. Mazzeo, S. Morin, A. Stokes, and F. Ilievski, "Multigait soft robot," *Proc. Natl Acad. Sci. USA*, vol. 108, pp. 20 400–20 403, 2011.

[5] Y. Hasegawa, Y. Mikami, K. Watanabe, and Y. Sankai, "Five-fingered assistive hand with mechanical compliance of human finger," in *2008 IEEE international conference on robotics and automation*. IEEE, 2008, pp. 718–724.

[6] H. Zhao, J. Jalving, R. Huang, R. Knepper, A. Ruina, and R. Shepherd, "A helping hand," *IEEE ROBOTICS & AUTOMATION MAGAZINE*, 2016.

[7] H. Zhao, K. O'Brien, S. Li, and R. F. Shepherd, "Optoelectronically innervated soft prosthetic hand via stretchable optical waveguides," *Science robotics*, vol. 1, no. 1, p. eaai7529, 2016.

[8] I. Van Meerbeek, C. De Sa, and R. Shepherd, "Soft optoelectronic sensory foams with proprioception," *Science Robotics*, vol. 3, no. 24, p. eaau2489, 2018.

[9] B. Jamil, G. Yoo, Y. Choi, and H. Rodrigue, "Proprioceptive soft pneumatic gripper for extreme environments using hybrid optical fibers," *IEEE Robotics and Automation Letters*, vol. 6, no. 4, pp. 8694–8701, 2021.

[10] H. Godaba, I. Vitanov, F. Aljaber, A. Ataka, and K. Althoefer, "A bending sensor insensitive to pressure: soft proprioception based on abraded optical fibres," in *2020 3rd IEEE International Conference on Soft Robotics (RoboSoft)*. IEEE, 2020, pp. 104–109.

[11] B. Mosadegh, P. Polygerinos, C. Keplinger, S. Wennstedt, R. F. Shepherd, U. Gupta, J. Shim, K. Bertoldi, C. J. Walsh, and G. M. Whitesides, "Pneumatic networks for soft robotics that actuate rapidly," *Advanced functional materials*, vol. 24, no. 15, pp. 2163–2170, 2014.

[12] P. Polygerinos, S. Lyne, Z. Wang, L. F. Nicolini, B. Mosadegh, G. M. Whitesides, and C. J. Walsh, "Towards a soft pneumatic glove for hand rehabilitation," in *2013 IEEE/RSJ International Conference on Intelligent Robots and Systems*. IEEE, 2013, pp. 1512–1517.

[13] C. Shi, X. Luo, P. Qi, T. Li, S. Song, Z. Najdovski, T. Fukuda, and H. Ren, "Shape sensing techniques for continuum robots in minimally invasive surgery: A survey," *IEEE Transactions on Biomedical Engineering*, vol. 64, no. 8, pp. 1665–1678, 2016.

[14] K. R. Henken, J. Dankelman, J. J. van den Dobbelsteen, L. K. Cheng, and M. S. van der Heiden, "Error analysis of fbg-based shape sensors for medical needle tracking," *IEEE/ASME Transactions on mechatronics*, vol. 19, no. 5, pp. 1523–1531, 2013.

[15] A. Hassan, F. Aljaber, H. Godaba, I. Vitanov, and K. Althoefer, "Soft multi-point waveguide sensor for proprioception and extereoception in inflatable fingers," in *2021 IEEE 6th International Forum on Research and Technology for Society and Industry (RTSI)*. IEEE, 2021, pp. 574–579.

[16] F. Aljaber, A. Hassan, I. Vitanov, and K. Althoefer, "Curvature and contact sensing with optical waveguides for soft silicone pneumatic actuator," in *2022 IEEE 5th International Conference on Soft Robotics (RoboSoft)*. IEEE, 2022, pp. 859–864.

[17] A. Hassan, F. Aljaber, I. Vitanov, and K. Althoefer, "Performance evaluation and optimisation of multi-point waveguide based optical sensor for soft robots," in *2022 IEEE International Conference on Flexible and Printable Sensors and Systems (FLEPS)*. IEEE, 2022, pp. 1–4.

[18] B. Mosadegh, P. Polygerinos, C. Keplinger, S. Wennstedt, R. F. Shepherd, U. Gupta, J. Shim, K. Bertoldi, C. J. Walsh, and G. M. Whitesides, "Soft robotics: pneumatic networks for soft robotics that actuate rapidly (adv. funct. mater. 15/2014)," *Advanced Functional Materials*, vol. 24, no. 15, pp. 2109–2109, 2014.

[19] H. Wang, M. Totaro, and L. Beccai, "Toward perceptive soft robots: Progress and challenges," *Advanced Science*, vol. 5, no. 9, p. 1800541, 2018.